Penerbit Akademia Baru

Journal of Advanced Research in Micro and Nano Engineering

Journal homepage:
https://www.akademiabaru.com/submit/index.php/armne/index
ISSN: 2756-8210

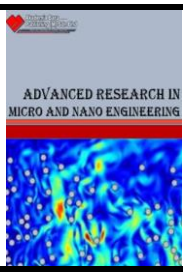

Identification and Analysis of Micro-Doppler Signature of a Bird Versus Micro-UAV

Siti Aminah Zulkarnain[1], Safiah Zulkifli[1,*], 'Aiffah Mohd Ali[1]

[1] School of Aerospace Engineering Campus, Universiti Sains Malaysia, 14300 Nibong Tebal, Pulau Pinang, Malaysia

ARTICLE INFO

Article history:
Received 30 October 2023
Received in revised form 13 December 2023
Accepted 25 January 2024
Available online 29 February 2024

Keywords:
Micro-UAVs; Micro-Doppler signature; radar application; CW radar; time-frequency analysis

ABSTRACT

The groundbreaking advancement of micro unmanned aerial vehicles (micro-UAVs) has been staggering. The diversity of micro-UAV operations is demanding in most sectors. However, the current regulatory framework for the civilian use of these devices is still insufficient. The operation of micro-UAVs may pose risks, including privacy violations and collision hazards. To address these concerns, a radar with advanced processing is needed. This study presents a preliminary design of an S-band continuous wave (CW) radar, which was simulated using MATLAB. The size of the rotating propeller blades of the micro-UAV ranges from 20 to 40 cm in length, while the size of a bird's flapping wing measures 35 cm in length, comprising 22 cm for the upper arm and 13 cm for the lower arm. The analysis was conducted under hovering conditions, where the target's main body is stationary while its micro-parts move continuously. The Short-Time Fourier Transform (STFT) analysis successfully identified the unique signature of both targets. The results showed that the S-band CW radar design at 5 GHz is effective in extracting the micro-Doppler signature of a bird versus a micro-UAV. The extracted features can be used as additional characteristics for target classification in the future.

1. Introduction

In recent years, micro-UAVs have become increasingly popular for various applications, both institutional and personal. However, this increase in usage has led to a growing risk of illegal activity [1-3]. Security control is thus a critical concern, and it is necessary to have technology designed specifically for micro-UAV detection and tracking in the airspace [4]. Deployable micro-UAVs on a large scale have raised concerns among authorities and communities. A detection system is required that can differentiate between micro-UAVs and birds to minimize false alarms generated by other objects in the airspace. This is because birds and micro-UAVs have similar Radar Cross Section (RCS) and speed, making it difficult for sensors to distinguish between them [5,6]. To improve the intelligence of the security system to detect and classify micro-UAV targets, an alternative approach for micro-UAV identification utilizing continuous wave radar is presented.

* *Corresponding author.*
E-mail address: safiahzul@usm.my

https://doi.org/10.37934/armne.16.1.102113

Sensor-based technology is used for detection, and there are different types of sensors available, including cameras [7], light detection and ranging (LIDAR) [8,9], sound sensors [10-12], and radar [13-15]. While cameras have the ability to capture images, they are limited in resolution, making them difficult to apply at high altitudes. LIDAR detection has some improvements, but it is expensive and limited in battery capacity and area size.

Radar sensors offer a significant approach to drone detection due to their operational range and ability to measure moving targets. Radar can be pulse or continuous wave form-based. Pulse radar can work at longer distances [16-18], but it has blind spots and requires high transmitting power. Continuous-wave radar continuously emits and receives electromagnetic waves and has no blind spots, making it practical for short-range sensing [19,20].

The micro-doppler (m-D) signature has been used to classify micro-UAVs and birds [21-23]. The moving part of the target causes frequency modulations on the backscattered echo waves, which result in distinct signatures depending on the target movements. Detailed Doppler characteristics can be extracted [24-27], enabling the radar to discriminate between micro-UAVs and birds. Spectrogram analysis is used for this purpose.

In the field of radar-based target identification, a noticeable gap exists in the comprehensive analysis of m-D signatures to discriminate between birds and micro-UAVs. While prior research has made strides in characterizing the m-D signatures of various targets, the specific differentiation between avian species and micro-UAVs remains largely unexplored. This gap in knowledge is particularly significant in the context of wildlife monitoring, airspace security, and drone regulation. Understanding the unique m-D patterns generated by birds and micro-UAVs is crucial for enhancing the accuracy and reliability of radar-based surveillance systems. Moreover, such insights can inform the development of more effective countermeasures against potential threats posed by UAVs and help mitigate the impact of UAVs on avian populations. Therefore, this study aims to bridge this gap by providing a comprehensive analysis of m-D signatures with specific objectives:

i. Develop a CW radar model using MATLAB programming to manage both transmitting and received signals.
ii. Investigate the radar signals reflected back from both micro-UAVs and birds.
iii. Extract distinctive characteristics from the m-D signatures with the aim of classifying targets.

These objectives guide our research efforts towards a better understanding of m-D signatures and their application in differentiating between birds and micro-UAVs, ultimately contributing to advancements in radar-based target identification technology and its practical use.

In pursuit of these objectives, the research methodology for obtaining the m-D signature with a CW radar model in a MATLAB simulation is described in detail in Section 2. Section 3 presents the simulation results, which effectively illustrate the proposed method's capabilities and outcomes. Finally, in section 4 concludes the paper and presents future works.

2. Methodology

The primary concept of micro-UAV detection involves using a sensor to detect and identify objects in shared airspace. This section outlines the working process of CW radar and how it can be used to detect a target. To investigate the radar's capability to detect a specific target, we will discuss the use of a MATLAB simulation for an S-band CW radar. Specifically, we will compare the detection of two targets: the rotating propeller blades of a micro-UAV and the flapping wings of a bird.

2.1 CW Radar Analysis

In micro-UAV detection, a sensor is utilized to detect objects within the shared airspace. To accomplish this, S-band CW radar is employed to emit radio waves, which are reflected or scattered when they contact an object. The transmitted signal, $S_T(t)$, and the received signal, $S_R(t)$, are expressed in Eq. (1) and Eq. (2), respectively.

$$S_T(t) = Ae^{j2\pi f_0 \mathrm{t}} \tag{1}$$

$$S_R(t) = Ae^{j2\pi f_0 (\mathrm{t}-\mathrm{t}_0)} \tag{2}$$

Here, A is the amplitude signal, f_0 is the carrier frequency of 5 GHz, and t_0 is the time delay. The signal is sampled with a 100 kHz sampling frequency, F_s, over an integration time, T, of 5 ms. The sampling period, T_s, is inversely proportional to F_s. To shift the signal's spectrum from f_0 to 0 Hz, the received signal is multiplied by $e^{-j2\pi f_0 \mathrm{t}}$. The time delay, t_0, can be calculated as the round-trip of the signal from the transmitter to the target and back to the receiver, as shown in Eq. (3)

$$t_0 = \frac{2R_0}{c} \tag{3}$$

where R_0 is the initial range of the target and c is the speed of light.

$$S_R(t) = Ae^{j2\pi f_0 \left(t-\frac{2R_0}{\mathrm{c}}\right)} \tag{4}$$

However, the use of advanced processing radar in this research needs to replace R_0 with $r(t)$ which is focused on the rotation of the rotor blade and flapping wing. Practically, most traditional radar systems focus on R_0 as mentioned in Eq. (4) and not all radars focus on $r(t)$. Due to this matter, it failed to differentiate the target.

$$S_R(t) = Ae^{j2\pi f_0 \left(t-\frac{2r(t)}{\mathrm{c}}\right)} \tag{5}$$

The m-D technique cooperates with $r(t)$ as stated in the Eq. (5).

2.2 The Mathematical Model for Propeller Blade

To assess the kinematics of micro-UAV with the operating radar, a model-simplifying assumption has been made regarding the primary body, which is assumed to be stationary while the propeller blades move uniformly. The model classification is based on the degree of dissimilarity in the m-D properties of rotational motion. Two coordinate systems, a fixed space coordinate system (X, Y) and a fixed object coordinate system (x, y) that are parallel to each other, have been established. The radar and propeller centers are located at the initial point of the two-coordinate system respectively.

As the radar remains stationary while the target is in motion, with both translational and rotational velocity. The rotational velocity is represented by the symbol ω_r, while the symbol v represents the translational velocity. The target's initial distance from the radar is denoted as R_0, and the time is denoted as t. The length of the propeller blade is L_2. Figure 1 illustrates the time-varying distance $r(t)$ between the antenna and S_2, which revolves around S_1.

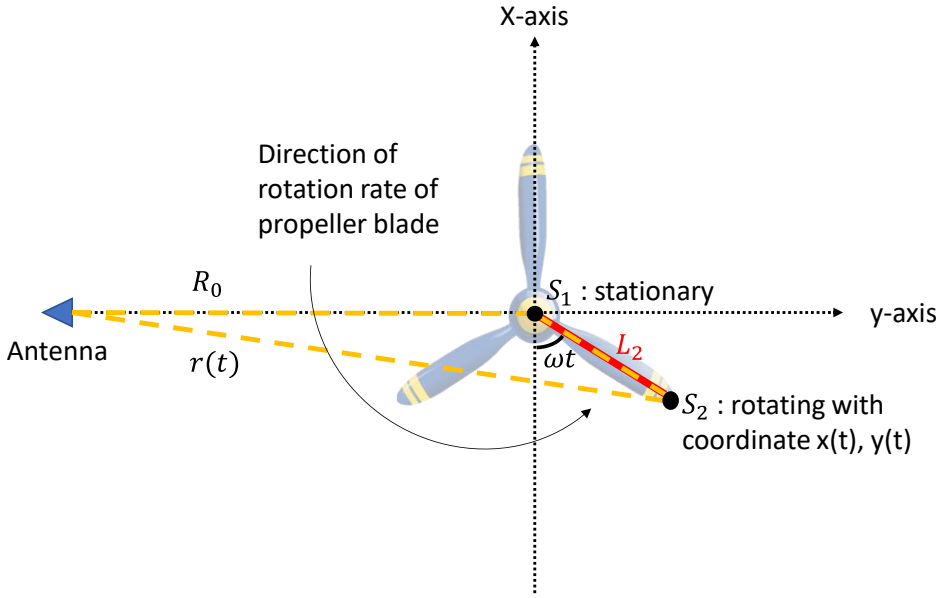

Fig. 1. The kinematic mechanism of radar system with a rotating propeller blade

The x-component and y-component motions, which are the breakdown of movement components used to determine the entire range of the propeller blade. The x-component of the target only accounts for rotational movement, as shown in Eq. (6)

$$\sum BladeX = L_2 cos(\omega_r t) \tag{6}$$

On the other hand, the y-component of the target consists of the starting range, the target's translational movement, and the y -component of rotational motion, as demonstrated in Eq. (7)

$$\sum BladeY = R_0 + vt + L_2 \sin(\omega_r t) \tag{7}$$

The total distance between the radar and the target is calculated using the Pythagorean theorem for both components, as demonstrated in Eq. (8)

$$r(t) = \sqrt{(\sum BladeX)^2 + (\sum BladeY)^2} \tag{8}$$

2.3 The Mathematical Model for Flapping Bird's Wing

The motion of a bird with flapping wings is a common example of a non-rigid target with joints. The kinematic model of a bird's flapping wing shows that the wing has two interdependent components, the elbow joint and the wrist joint. In Figure 2, the lower arm connects to the wingtip at the wrist joint, while the upper arm connects to the lower arm at the elbow joint. The wrist joint can rotate and swing along two vertical axes of motion, while the elbow joint can only move up and down on a fixed plane.

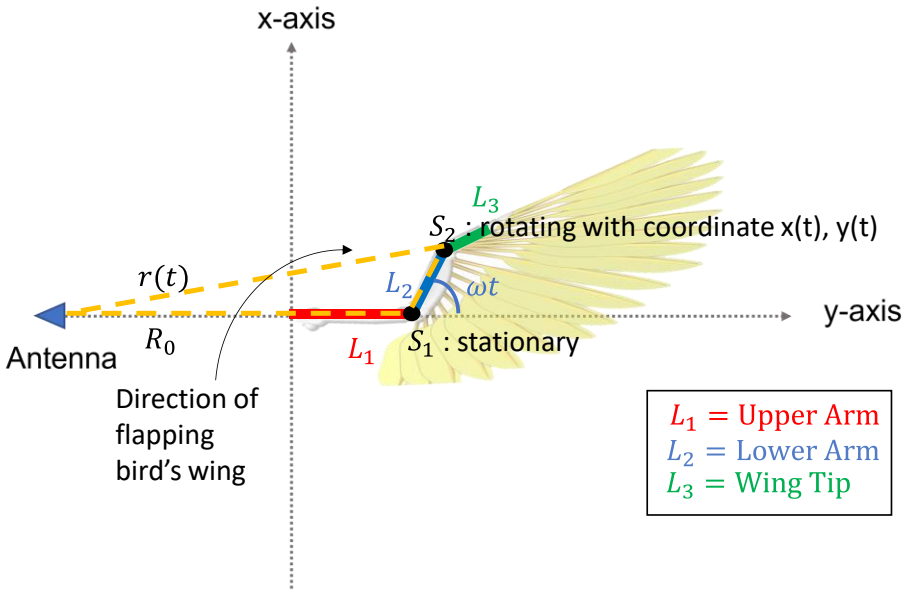

Fig. 2. The kinematic mechanism of radar system utilizing a flapping bird's wing

To simplify the modelling process, the wingtip L_3 is disregarded, and it is assumed that the upper arm L_1 is largely immobile at the point S_1, while the lower arm L_2 is flapping at a point S_2. The scattering point in the lower arm L_2 oscillates, while the flapping wing target travels with an angular velocity of bird wing ω. The angular and linear velocities of the target can be determined using Eq. (9) and Eq. (10)

$$\omega = 2\pi f_{flap} \tag{9}$$

$$v = -2(L_1 + L_2)\pi A f_{flap} \sin(\omega t) \tag{10}$$

where f_{flap} is the lower arm's flapping frequency. A is the lower arm's flapping amplitude, and L_1 and L_2 represent the lengths of the upper and lower arm, respectively. Eq. (11) provides a mathematical representation of the total range of the flapping wing target, incorporating both the linear motion and the range oscillation. It allows for the calculation of the target's position in terms of range at a specific time in the simplified model. It can be expressed as

$$Total\ r(t) = R_0 + vt + \omega t \sin(\omega t) \tag{11}$$

Here, $Total\ r(t)$ represents the total range at a given time, R_0 is the initial range, vt accounts for the linear motion of the target, and $\omega t \sin(\omega t)$ describes the range oscillation.

2.4 Signal-Processing

The overlapping Fast Fourier Transform (FFT) applied to each range bin of a time domain signal is a crucial measurement method for obtaining a spectrogram. This method converts a signal into spectral components, providing frequency information about the signal. To begin this process, a portion of the signal is received and stored in memory for further processing. The sampling frequency of the radar system is denoted by $F_s = 1/T_s$, with the "Nyquist frequency" equal to half the value of

F_s. According to the Nyquist theorem, F_s must be at least double the highest frequency signal to accurately measure the sample. The frequency resolution is determined by selecting the FFT length.

For non-stationary signals, the STFT is a time-frequency analysis technique that is employed. STFT separates a time-domain input signal into overlapping frames by multiplying the signal with a window function and then applying the FFT to each frame. The window function's length in the STFT is related to the signal's resolution. Longer windows offer higher frequency resolution but lower time resolution, while shorter windows provide higher time resolution but lower frequency resolution.

3. Results

In this section, the outcomes derived from the processed and analysed MATLAB data are presented and discussed. A sampling frequency of 100 kHz and an integration time of 700 ms were used to sample the signal, where the sampling frequency and integration time are denoted by F_s and T, respectively. The selection of the 5 GHz frequency range for this study took into account budget limitations. Although it is generally true that lower frequency ranges necessitate larger and costlier antennas, it should be emphasized that not all components related to higher frequency ranges are less expensive. In fact, higher frequency ranges may require a substantial budget allocation for the procurement of other associated components. However, it remains accurate to state that antennas designed for higher frequency ranges are typically less expensive due to their smaller physical dimensions. Figure 3 displays the frequency spectra of the signals, with the frequency span ranging from -50 kHz to 50 kHz due to the sampling frequency of 100 kHz. A spike at 0 Hz frequency Doppler indicates that the target is stationary, as illustrated in Figure 3.

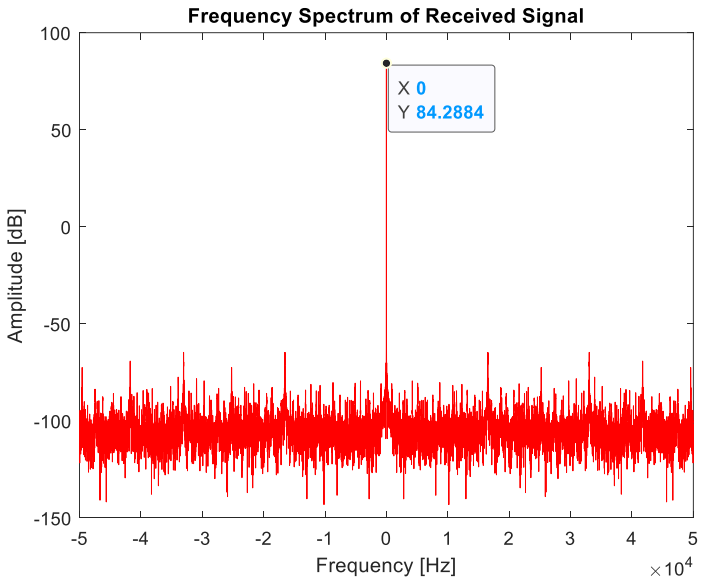

Fig. 3. The frequency spectrum of the receiving signal

3.1 M-D Analysis of Rotating Propeller Blade

In addition to the FFT and Doppler distribution analysis, the Short-Time Fourier Transform (STFT) is also employed to study the propeller blade's rotational characteristics. Figure 4(a) presents the FFT graph, which shares the same 700 ms duration as the STFT graph in Figure 4(b). The STFT spectrogram showcases a trade-off between time and frequency resolution. By using a window length of 100, the STFT achieves a finer frequency resolution but at the expense of coarser time resolution.

This behaviour is observed due to the dispersion of signal energy along the time axis and the compactness along the frequency axis in the STFT spectrogram. The shorter window length allows for more precise frequency information, allowing us to discern finer details of the propeller blade's rotational rate. However, this comes at the cost of reduced time resolution, as the shorter window length covers a smaller portion of the overall time duration.

When examining the Figure 4(a), the doppler distribution value at -3159.95 Hz and 3159.95 Hz still holds significant information about the propeller blade's rotational rate, just as in the STFT analysis. Expanding upon the analysis, at v=0 m/s, the Doppler distribution in Figure 4(b) exhibits the same interesting symmetry observed in the FFT graph. The distribution is equal at both the negative and positive sides of the graph. This symmetry arises because when the target is hovering, there is no relative motion between the target and the sensor. Consequently, the reflected signal experiences an equal but opposite frequency shift compared to the transmitted signal.

By incorporating the STFT analysis and discussing its characteristics alongside the FFT and Doppler distribution, a comprehensive understanding of the propeller blade's rotational behaviour can be obtained.

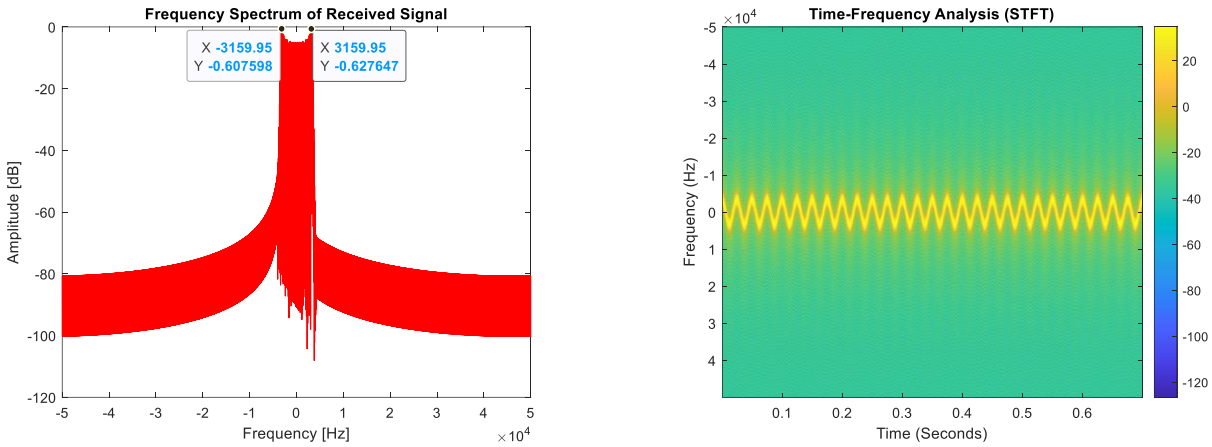

(a) (b)

Fig. 4. The m-D analysis of a micro-UAV shows (a) the FFT analysis of the propeller blade, and (b) the STFT analysis of the propeller blade

3.2 M-D Analysis of Flapping Bird

Figure 5(a) shows significant dispersion when the flapping frequency (fflap) is set to 5 Hz. In this analysis, a Fast Fourier Transform (FFT) is applied to the signal obtained from the flapping bird, with a sampling frequency of 100 kHz, meaning that 100,000 samples are acquired per second. An integration time of 700 ms is used to enhance the signal quality and reduce noise.

The dispersion observed in Figure 5(a) indicates that the frequencies present in the signal are spread out or distributed over a wide range. This dispersion can be attributed to the flapping motion of the bird at a frequency of 5 Hz. As the bird flaps its wings, it generates a varying Doppler shift in the reflected signal. This Doppler shift introduces a range of frequencies in the received signal, resulting in dispersion in the FFT graph. The significant dispersion observed in Figure 5(a) suggests that the flapping motion of the bird at 5 Hz contributes to a wide range of frequency components in the received signal. This dispersion can provide valuable information about the flapping bird's motion and characteristics, allowing for further analysis and interpretation of its behaviour.

However, instead of calculating a single FFT on the entire signal, the STFT divides the signal into smaller segments or time windows and performs FFT on each window. This allows capturing the

signal's frequency content and how it varies over time. Figure 5(b) represents the STFT analysis for the flapping bird with a flapping frequency of 5 Hz. It illustrates how the frequency content of the signal changes over time. Each point in the graph corresponds to a specific time-frequency bin and represents the magnitude or power of the frequency components at that particular time and frequency.

By observing Figure 5(b), one can analyse the time-varying characteristics of the bird's m-D signature. The STFT analysis provides insights into how the frequency components change as the bird flaps its wings. It may reveal patterns, trends, or distinctive features related to the bird's motion or other characteristics.

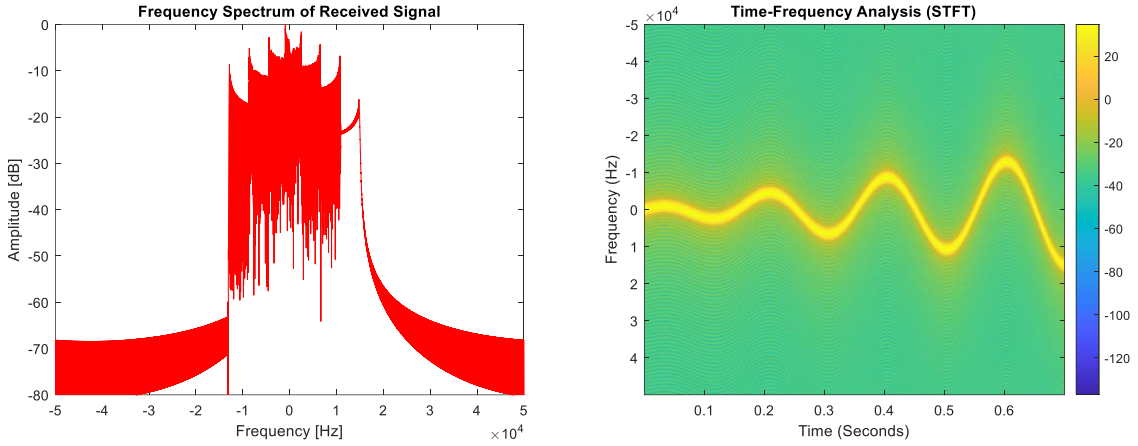

(a) (b)

Fig. 5. The m-D analysis of a bird shows (a) the FFT analysis of the bird wing, and (b) the STFT analysis of the bird wing

3.3 Various Model Properties & Variables

In the conducted analysis, both FFT and STFT techniques were employed to examine the m-D signature induced by varying lengths of propeller blades on micro-UAVs. The micro-UAV target was equipped with two sets of propeller blades, one measuring 20 cm and the other 30 cm in length, rotating at a fixed rate of 40 rotations per second (rps), equivalent to an angular velocity of approximately 80π rad/s. The results of the FFT analysis, presented in Figure 6, displayed a doppler distribution for the 20 cm propeller blade, with lines separated by approximately -1519.98 Hz and 1519.98 Hz.

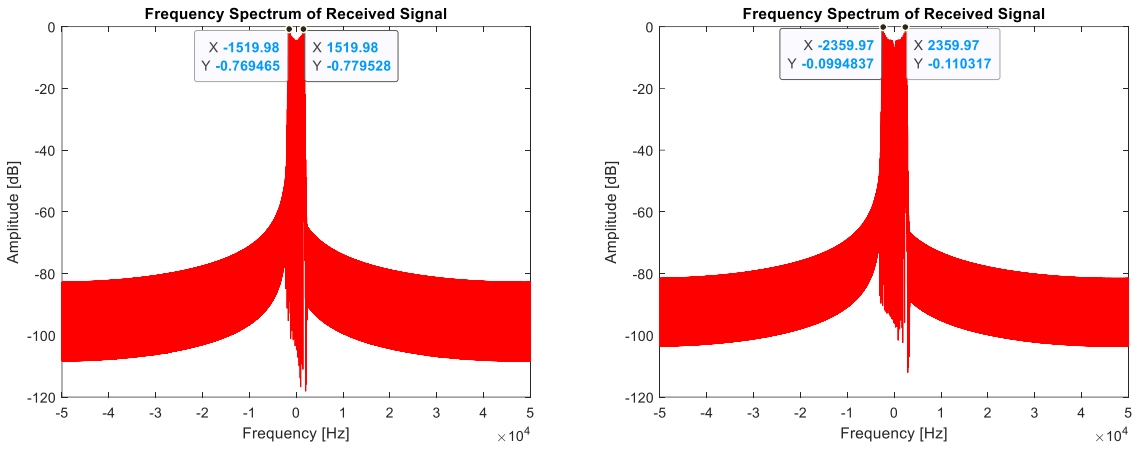

(a) (b)

Fig. 6. The FFT analysis of the micro-UAVs at (a) 20 cm (b) 30 cm length of propeller blade

In comparison, the doppler distribution observed for the 30 cm propeller blade, depicted in Figure 7, exhibited lines separated by approximately -2359.97 Hz and 2359.97 Hz. These doppler distributions provided insights into the rotation rates of the respective propeller blades. Furthermore, the STFT analysis was conducted to explore the m-D signature characteristics in more detail. The collected data was digitized at a sampling frequency of 100 kHz, resulting in a total of 100 kiloSamples and a measurement duration of 700 ms. The window length of 100 was utilized to extract the m-D signature. The results of the STFT analysis demonstrated that the periodical sinusoidal signature of the 30 cm propeller blade was more distinct and well-defined compared to the 20 cm propeller blade. The STFT plot revealed that larger propeller blades exhibited a higher separation between lines, indicating a clearer representation of the frequency components associated with the propeller blade's rotation rate.

By combining the insights from the FFT and STFT analyses, a comprehensive understanding of the effects of propeller blade length on the micro-UAV's m-D signature can be obtained, enabling improved detection and characterization of the target. Two different model properties and variables were considered for both micro-UAVs and birds in this study. The first model aimed to investigate the detection of the m-D signature induced by varying lengths of propeller blades, while the second model aimed to explore the detection of the m-D signature induced by different lengths of the bird's lower arm.

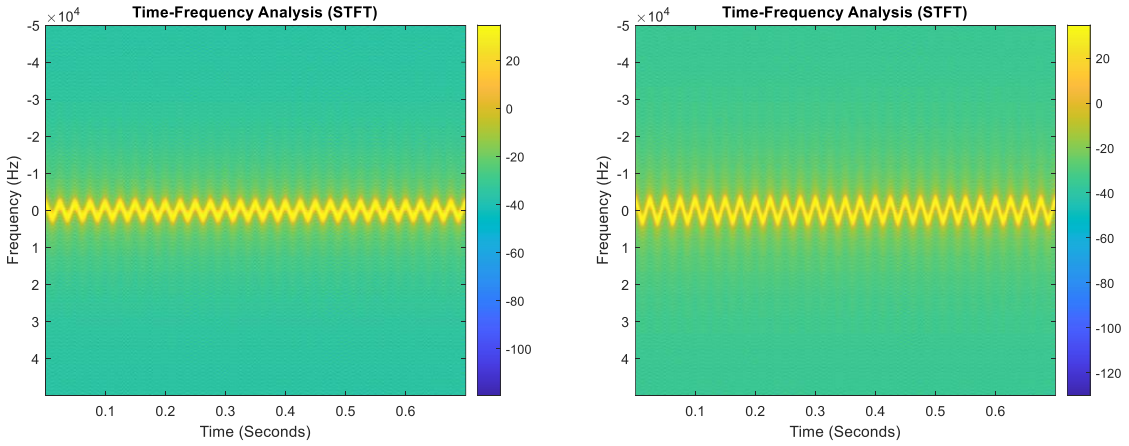

(a) (b)

Fig. 7. The STFT analysis of the micro-UAVs at (a) 20 cm and (b) 30 cm length of propeller blade

The next model investigated in this study focuses on a bird target with flapping frequencies of 3 Hz and 4 Hz. To analyse the m-D signature induced by the bird's wing motion, data was collected at a sampling frequency of 100 kHz, resulting in 100,000 samples or a duration of 700 ms for each signature. Figure 8 presents the FFT spectrograms of the bird wing, providing insights into the frequency components associated with different flapping frequencies. The spectrograms illustrate the time-varying frequency content of the radar signal, allowing for a detailed examination of the bird's flight dynamics. The FFT spectrogram for the 3 Hz flapping frequency exhibits a more localized and concentrated distribution of frequency content compared to the 4 Hz flapping frequency. This suggests a relatively stable and consistent flapping motion over time at 3 Hz. Conversely, the FFT spectrogram for the 4 Hz flapping frequency shows a wider spread of frequency components, indicating a more varied and dynamic wing motion.

In addition to the FFT analysis, the STFT analysis was conducted to further explore the m-D signature of the bird target with flapping frequencies of 3 Hz and 4 Hz. The STFT analysis allows for a more detailed examination of the frequency content over time. The collected data, digitized at a sampling frequency of 100 kHz, provided a high-resolution representation of the bird's wing motion.

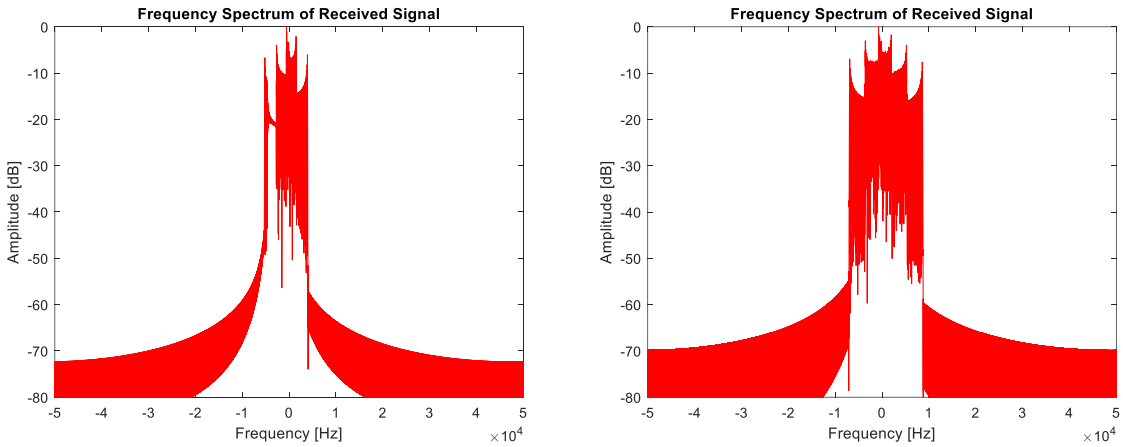

(a) (b)

Fig. 8. The FFT analysis of the bird wing at (a) 3 Hz and (b) 4 Hz flapping frequency

Figure 9 displays the STFT spectrograms for the bird wing at the two different flapping frequencies. The STFT spectrograms illustrate the time-varying frequency components of the radar signal, providing a comprehensive view of the bird's flight dynamics. For the 3 Hz flapping frequency, the STFT spectrogram exhibits a more localized and concentrated distribution of frequency content, indicating a relatively stable and consistent flapping motion over time. Conversely, the STFT spectrogram for the 4 Hz flapping frequency shows a wider spread of frequency components, indicating a more varied and dynamic wing motion.

The STFT analysis enhances our understanding of the bird's m-D signature by capturing the temporal variations in frequency content. It allows for the identification of different phases in the bird's flapping cycle and provides insights into the timing and duration of specific frequency components associated with the wing motion. By comparing the FFT spectrograms and the STFT spectrograms for different flapping frequencies, we can distinguish patterns and characteristics that are unique to each frequency, contributing to the overall radar signature of the bird.

Combining the findings from the FFT analysis and the STFT analysis provides a comprehensive analysis of the m-D signature induced by the bird's wing motion at 3 Hz and 4 Hz. These insights contribute to the understanding of the bird's flight behaviour, aiding in the effective detection, identification, and tracking of avian targets in radar systems.

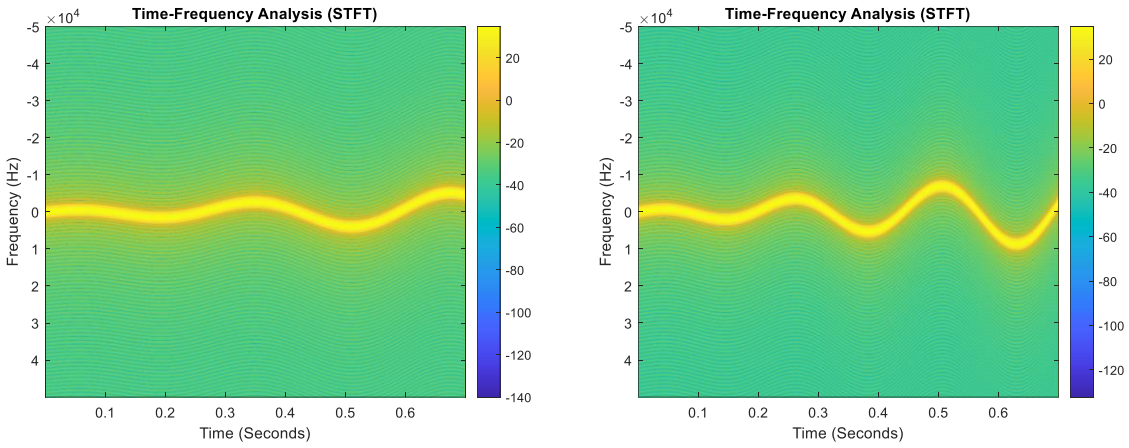

(a) (b)

Fig. 9. The STFT analysis of the bird wing at (a) 3 Hz and (b) 4 Hz flapping frequency

4. Conclusions

A MATLAB simulation was used to investigate the preliminary design of an S-band CW radar. The motivation behind this study was to address the growing problem of illegal and harmful activities involving micro-UAVs. The study compared two cases: the rotating propeller blades of a micro-UAV and the flapping wings of a bird. The results suggest that an S-band CW radar at 5 GHz is an effective means of detecting the m-D signatures of both targets, which may pose a challenge for conventional radars. The STFT method was used to successfully distinguish the unique signatures of both targets, and the results were consistent with previous research. Mathematical models of both targets were employed to better understand the kinematic mechanism of the radar with respect to the target. Further research should be carried out to apply these findings and enhance the detection capabilities of radar. However, it is crucial to conduct further research and analysis to fully assess the practical impact and potential benefits of these enhancements in improving radar's detection capabilities.

Acknowledgement

This research was supported by Universiti Sains Malaysia, Short-Term Grant with Project No:304/PAERO.6315627.

References

[1] Sandbrook, Chris. "The social implications of using drones for biodiversity conservation." *Ambio* 44, no. Suppl 4 (2015): 636-647. https://doi.org/10.1007/s13280-015-0714-0

[2] Chang, Victoria, Pramod Chundury, and Marshini Chetty. "Spiders in the sky: User perceptions of drones, privacy, and security." In *Proceedings of the 2017 CHI conference on human factors in computing systems*, pp. 6765-6776. 2017. https://doi.org/10.1145/3025453.3025632

[3] Aydin, Burchan. "Public acceptance of drones: Knowledge, attitudes, and practice." *Technology in society* 59 (2019): 101180. https://doi.org/10.1016/j.techsoc.2019.101180

[4] Merkert, Rico, and James Bushell. "Managing the drone revolution: A systematic literature review into the current use of airborne drones and future strategic directions for their effective control." *Journal of air transport management* 89 (2020): 101929. https://doi.org/10.1016/j.jairtraman.2020.101929

[5] Gong, Jiangkun, Jun Yan, Deren Li, Deyong Kong, and Huiping Hu. "Interference of radar detection of drones by birds." *Progress In Electromagnetics Research M* 81 (2019): 1-11. https://doi.org/10.2528/PIERM19020505

[6] Alabaster, Clive M., Evan J. Hughes, and Dan W. Forman. "Is it a bird or is it a plane?." In *2012 International Waveform Diversity & Design Conference (WDD)*, pp. 007-012. IEEE, 2012. https://doi.org/10.1109/WDD.2012.7311311

[7] Seidaliyeva, Ulzhalgas, Daryn Akhmetov, Lyazzat Ilipbayeva, and Eric T. Matson. "Real-time and accurate drone detection in a video with a static background." *Sensors* 20, no. 14 (2020): 3856. https://doi.org/10.3390/s20143856

[8] Salhi, Meriem, and Noureddine Boudriga. "Multi-array spherical LiDAR system for drone detection." In *2020 22nd International Conference on Transparent Optical Networks (ICTON)*, pp. 1-5. IEEE, 2020. https://doi.org/10.1109/ICTON51198.2020.9203381
[9] Dogru, Sedat, and Lino Marques. "Drone detection using sparse lidar measurements." *IEEE Robotics and Automation Letters* 7, no. 2 (2022): 3062-3069. https://doi.org/10.1109/LRA.2022.3145498
[10] Jamil, Sonain, Fawad, MuhibUr Rahman, Amin Ullah, Salman Badnava, Masoud Forsat, and Seyed Sajad Mirjavadi. "Malicious UAV detection using integrated audio and visual features for public safety applications." *Sensors* 20, no. 14 (2020): 3923. https://doi.org/10.3390/s20143923
[11] Busset, Joël, Florian Perrodin, Peter Wellig, Beat Ott, Kurt Heutschi, Torben Rühl, and Thomas Nussbaumer. "Detection and tracking of drones using advanced acoustic cameras." In *Unmanned/Unattended Sensors and Sensor Networks XI; and Advanced Free-Space Optical Communication Techniques and Applications*, vol. 9647, pp. 53-60. SPIE, 2015. https://doi.org/10.1117/12.2194309
[12] Dumitrescu, Cătălin, Marius Minea, Ilona Mădălina Costea, Ionut Cosmin Chiva, and Augustin Semenescu. "Development of an acoustic system for UAV detection." *Sensors* 20, no. 17 (2020): 4870. https://doi.org/10.3390/s20174870
[13] Caris, Michael, Stephan Stanko, Winfried Johannes, Stefan Sieger, and Nils Pohl. "Detection and tracking of Micro Aerial Vehicles with millimeter wave radar." In *2016 European Radar Conference (EuRAD)*, pp. 406-408. IEEE, 2016. https://doi.org/10.1109/EuMC.2016.7824653
[14] Jarabo-Amores, M. Pilar, David Mata-Moya, Pedro J. Gómez-del-Hoyo, J. L. Bárcena-Humanes, J. Rosado-Sanz, N. Rey-Maestre, and M. Rosa-Zurera. "Drone detection feasibility with passive radars." In *2018 15th European Radar Conference (EuRAD)*, pp. 313-316. IEEE, 2018. https://doi.org/10.23919/EuRAD.2018.8546549
[15] Jian, Michael, Zhenzhong Lu, and Victor C. Chen. "Drone detection and tracking based on phase-interferometric Doppler radar." In *2018 IEEE Radar Conference (RadarConf18)*, pp. 1146-1149. IEEE, 2018. https://doi.org/10.1109/RADAR.2018.8378723
[16] Kim, Byung-Kwan, Junhyeong Park, Seong-Jin Park, Tae-Wan Kim, Dae-Hwan Jung, Do-Hoon Kim, Taihyung Kim, and Seong-Ook Park. "Drone Detection with Chirp-Pulse Radar Based on Target Fluctuation Models." *ETRI journal* 40, no. 2 (2018): 188-196. https://doi.org/10.4218/etrij.2017-0090
[17] Salem, Sameh G., M. H. Hossiny, Fathy M. Ahmed, and K. H. Moustafa. "Hardware implementation of proposed CAMP algorithm for pulsed radar." *Journal of Advanced Research in Applied Mechanics* 45, no. 1 (2018): 20-30.
[18] Salem, Sameh G., M. H. Hossiny, Fathy M. Ahmed, and K. H. Moustafa. "Design and implementation of compressive sensing on pulsed radar." *Journal of Advanced Research in Applied Mechanics* 44, no. 1 (2018): 15-23.
[19] Mazumder, Joydeep, and Arockia Bazil Raj. "Detection and classification of UAV using propeller Doppler profiles for counter UAV systems." In *2020 5th International Conference on Communication and Electronics Systems (ICCES)*, pp. 221-227. IEEE, 2020. https://doi.org/10.1109/ICCES48766.2020.9138077
[20] Kumawat, Harish C., and Arockia Bazil Raj. "Extraction of Doppler signature of micro-to-macro rotations/motions using continuous wave radar-assisted measurement system." *IET Science, Measurement & Technology* 14, no. 7 (2020): 772-785. https://doi.org/10.1049/iet-smt.2018.5563
[21] Hoffmann, Folker, Matthew Ritchie, Francesco Fioranelli, Alexander Charlish, and Hugh Griffiths. "Micro-Doppler based detection and tracking of UAVs with multistatic radar." In *2016 IEEE radar conference (RadarConf)*, pp. 1-6. IEEE, 2016. https://doi.org/10.1109/RADAR.2016.7485236
[22] Molchanov, Pavlo, Ronny IA Harmanny, Jaco JM de Wit, Karen Egiazarian, and Jaakko Astola. "Classification of small UAVs and birds by micro-Doppler signatures." *International Journal of Microwave and Wireless Technologies* 6, no. 3-4 (2014): 435-444. https://doi.org/10.1017/S1759078714000282
[23] Rahman, Samiur, and Duncan A. Robertson. "Radar micro-Doppler signatures of drones and birds at K-band and W-band." *Scientific reports* 8, no. 1 (2018): 17396. https://doi.org/10.1038/s41598-018-35880-9
[24] Gong, Jiangkun, Jun Yan, Deren Li, Ruizhi Chen, Fengyi Tian, and Zhen Yan. "Theoretical and experimental analysis of radar micro-Doppler signature modulated by rotating blades of drones." *IEEE Antennas and Wireless Propagation Letters* 19, no. 10 (2020): 1659-1663. https://doi.org/10.1109/LAWP.2020.3013012
[25] Singh, Ashish Kumar, and Yong-Hoon Kim. "Automatic measurement of blade length and rotation rate of drone using W-band micro-Doppler radar." *IEEE Sensors Journal* 18, no. 5 (2017): 1895-1902. https://doi.org/10.1109/JSEN.2017.2785335
[26] Oh, Beom-Seok, Xin Guo, Fangyuan Wan, Kar-Ann Toh, and Zhiping Lin. "Micro-Doppler mini-UAV classification using empirical-mode decomposition features." *IEEE Geoscience and Remote Sensing Letters* 15, no. 2 (2017): 227-231. https://doi.org/10.1109/LGRS.2017.2781711
[27] Fuhrmann, Lars, Oliver Biallawons, Jens Klare, Reinhard Panhuber, Robert Klenke, and J. Ender. "Micro-Doppler analysis and classification of UAVs at Ka band." In *2017 18th International Radar Symposium (IRS)*, pp. 1-9. IEEE, 2017. https://doi.org/10.23919/IRS.2017.8008142